Available online at www.sciencedirect.com

ScienceDirect

Physics Procedia 69 (2015) 593 – 598

Physics Procedia

10 World Conference on Neutron Radiography 5-10 October 2014

Visualization of bubble behavior in a packed bed of spheres using neutron radiography

Daisuke Ito*, Yasushi Saito

Research Reactor Institute, Kyoto University, 2-1010 Asashiro-nishi, Kumatori, Sennan, Osaka 590-0494, Japan

Abstract

The present paper describes gas-liquid two-phase flow measurements in a packed bed of spheres using neutron radiography. Porous debris formed during a severe accident of a nuclear reactor should be cooled by a coolant and the cooling characteristics are dominated by two-phase flow behavior in the debris bed at the initial stage of the accident. Therefore, experimental database of the two-phase flow in the porous media has been required for safety analysis of the reactor. However, it is difficult to observe the flow structure, for example, void fraction distribution in such complex flow channel. In this study, the local void fraction in a packed bed which simulates the debris bed was measured by high frame-rate neutron radiography. Experiments were performed in air-water two-phase flow in a vertical pipe. Alumina spheres with 5 mm in diameter were packed randomly in the pipe. The bubble behavior between the spheres was investigated by using the void fraction distributions estimated from the neutron radiographs. Although it was difficult to track the small bubbles in the packed bed, the move of the large bubble could be found roughly from the distribution. In addition, the fluctuation of the void fraction was compared with that of the pressure drop in the test section. From these results, the possibility of the gas velocity estimation was shown.

Selection and peer-review under responsibility of Paul Scherrer Institut

Keywords: Air-water two-phase flow; debris bed; neutron radiography;void fraction; porosity

1. Introduction

Severe accident studies are very important for safety evaluation of nuclear reactors. There are a lot of issues to be solved in such study. Among them, fuel-coolant interaction (FCI) has to be clarified to understand the transient

* Corresponding author. Tel.: +81-72-451-2373; fax: +81-72-451-2431.
E-mail address: itod@rri.kyoto-u.ac.jp

Selection and peer-review under responsibility of Paul Scherrer Institut
doi:10.1016/j.phpro.2015.07.084

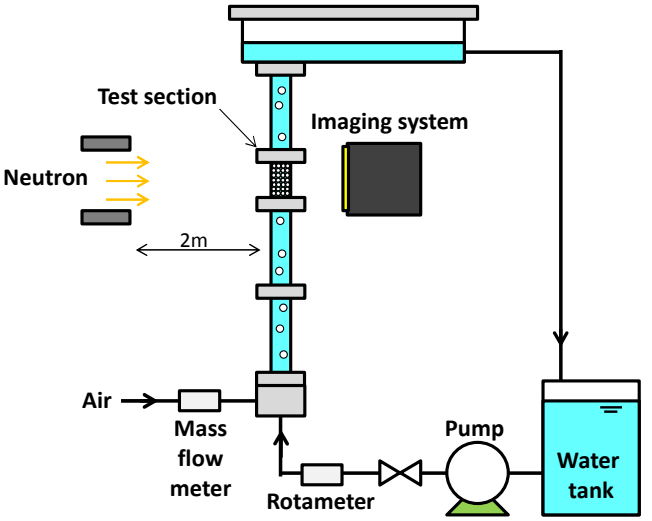

Fig. 1. Schematic layout of experimental setup.

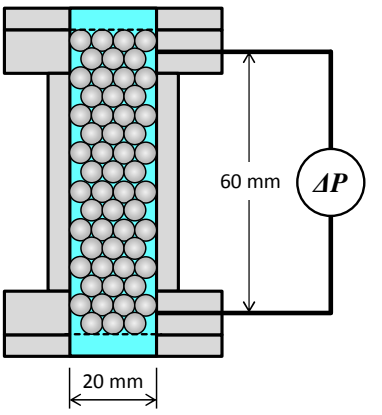

Fig. 2. Schematic view of test section.

behavior after fuel melting accident. The debris formed by molten fuel is a key to safety of the reactor and it should be cooled optimally. The cooling characteristics are dominated by gas-liquid two-phase flow behavior in the debris bed at the initial stage of the accident (Sehgal 2011). Recently, many numerical studies have contributed to analyze the flow behavior in the debris (Wang and Beckermann 1993, Duval et al. 2004). However, experimental database for the validation of the numerical results is not enough so far, because the debris bed has very complex flow channel and it is so difficult to measure the flow behavior inside it. Therefore, we applied a neutron radiography technique, which can measure two-dimensional void fraction distributions (Hibiki et al. 1994, Takenaka et al. 1996, Kureta et al. 2001), to visualize the two-phase flow structure in the debris. Since neutrons can pass through high density materials e.g. metals, it enables to evaluate two-phase flow dynamics in the debris bed experimentally. In the present study, two-phase flow in a sphere packed bed, which simulates the debris bed, is investigated by the high-frame rate neutron radiography and the experiments are carried out in air-water two-phase flow system. The distributions of the porosity and void fraction in the packed bed are estimated from the acquired radiographs and the two-phase flow behavior in the porous media is studied.

2. Experimental setup and method

Fig. 1 shows a schematic layout of the experimental setup for air-water two-phase flow measurement. The experiments are performed at the B-4 experimental room in the Kyoto University Research Reactor (Saito et al. 2011). This setup consists of a pump, an air-water mixing part, a test pipe, and a water tank. The vertical circular pipe has an inner diameter of 20 mm and it is made of aluminum. Water is circulated by the pump and compressed air is injected at the mixing part. Both water and air flow rates are monitored and the superficial gas and liquid velocities (J_G and J_L) are set by controlling the valves. Alumina spheres, 5 mm in diameter, are packed randomly in the test section, as illustrated in Fig. 2.

In the neutron radiography, transmitted neutrons are converted to optical light by a LiF:ZnS(Ag) converter and it is acquired by an imaging system with an image intensifier (single MCP (GaAsP) + booster) and a high speed camera (MotionPro Y4 Lite, IDT). The neutron flux at the beam exit is 5×10^7 n/cm^{2}s at 5 MW operation. The frame rate is set at 200 Hz to observe the dynamic behavior in the present experiments. The neutron radiographs have a pixel density of 0.16 mm/pixel and 10 bit gray levels. To obtain higher quality radiographs, the radiographs

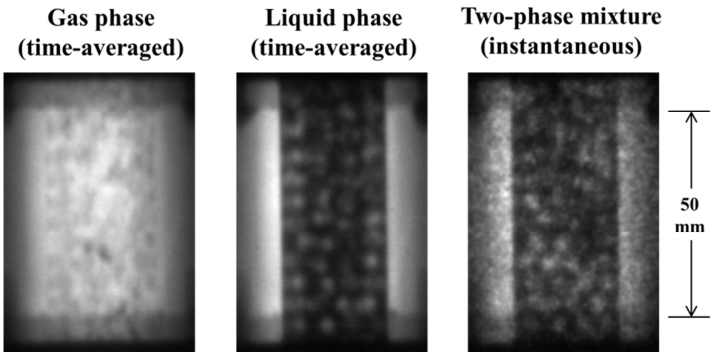

Fig. 3. Typical radiographs for the gas phase, the liquid phase and the two-phase mixture in the packed bed of spheres.

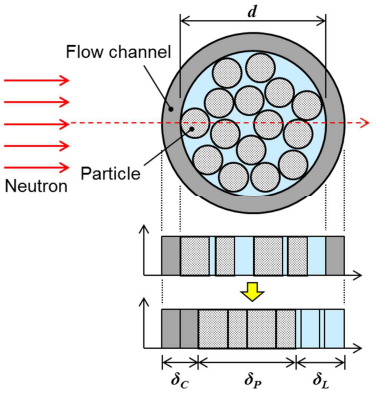

Fig. 4. Schematics of the thicknesses in the test section.

are post-processed and three-dimensional median filter is applied to the acquired image sequence. A pressure transducer (PA-838-101D, COPAL Electronics) is installed at the test section, as shown in Fig.2, and the time-series signal of the pressure drop in the sphere packed bed is measured simultaneously.

3. Experimental results

3.1. Estimations of porosity and void fraction in packed bed

Typical neutron radiographs acquired in the packed bed of the alumina spheres are shown in Fig. 3. Since the neutron attenuation coefficient of the alumina is low and water has higher value, the alumina spheres are visualized in these radiographs as voids. In the gas phase image, it is seen that the neutron beam is almost transmitted. In contrast, the neutrons attenuate significantly in the liquid phase. The pixel gray scale value of the radiograph of the sphere packed bed filled with gas phase (G_G), liquid phase (G_L) and two-phase mixture (G_{ML}) can be expressed by the following equations,

$$G_G = C \cdot \phi_{th} \cdot \exp\left(-\Sigma_T \delta_T\right) + G_0 \tag{1}$$

$$G_L = C \cdot \phi_{th} \cdot \exp\left(-\Sigma_T \delta_T - \Sigma_L \delta_L\right) + G_0 \tag{2}$$

$$G_{ML} = C \cdot \phi_{th} \cdot \exp\left(-\Sigma_T \delta_T - \Sigma_L \delta_{ML}\right) + G_0 \tag{3}$$

where G, C, ϕ_{th}, Σ and δ represent the image gray level, the gain, the thermal neutron flux, the total macroscopic cross section, and the thickness, respectively. The subscripts T, G, L and ML denote the test section, the gas single phase, the liquid single phase and the liquid phase in two-phase mixture, respectively. In the packed bed of the spheres, $\Sigma_T \delta_T$ is a sum of $\Sigma_C \delta_C$ for the flow channel and $\Sigma_P \delta_P$ for the packed particle, as shown in Fig. 4. The offset (G_0) includes the dark current component (G_D) of the imaging system and the neutron scattering component (G_S). However, in this experiment, since the amount of water in the test section is not a lot, the neutron scattering from water can be neglected.

$$G_0 = G_D + G_S \approx G_D \tag{4}$$

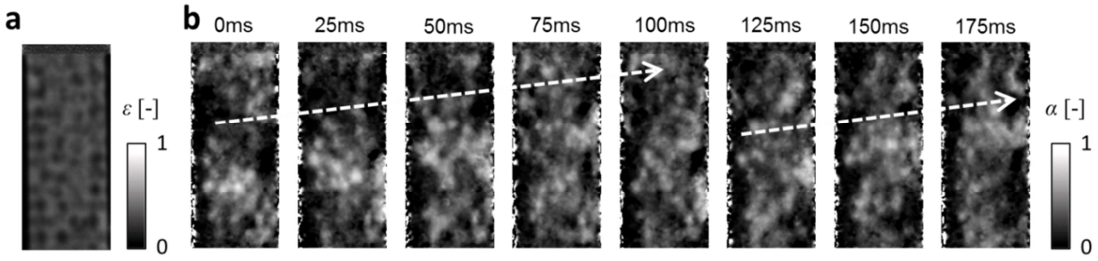

Fig. 5. Typical distributions of (a) porosity and (b) instantaneous void fraction.

Here, G_0 is assumed to be spatially constant. Then, the thickness of the liquid phase (δ_L) is calculated from Eq. (1) and Eq. (2), as follows,

$$\delta_L = -\frac{1}{\Sigma_L}\ln\left(\frac{G_L - G_0}{G_G - G_0}\right) \tag{5}$$

As a result, δ_L is obtained locally, and the local porosity (ε) of the porous media is estimated from the following equation.

$$\varepsilon = \frac{\delta_L}{d} \tag{6}$$

where d is the thickness of the test section, as shown in Fig.4. Therefore, the spatial distribution of the porosity can be estimated from the radiographs of the packed bed filled with gas or liquid phases by Eq. (5) and Eq. (6).

The thickness of the liquid phase in the two-phase mixture (δ_{ML}) is also calculated from the equations above, as follows,

$$\delta_{ML} = -\frac{1}{\Sigma_L}\ln\left(\frac{G_{ML} - G_0}{G_G - G_0}\right) \tag{7}$$

Thus, the local void fraction (α) is estimated from the radiographs of the gas and liquid phases and the two-phase mixture, as follow.

$$\alpha = 1 - \frac{\delta_{ML}}{\delta_L} = \ln\left(\frac{G_L - G_0}{G_{ML} - G_0}\right) \Big/ \ln\left(\frac{G_L - G_0}{G_G - G_0}\right) \tag{8}$$

3.2. Spatial distributions of porosity and void fraction

The estimated porosity distribution and typical sequence of the void fraction distributions are shown in Fig. 5. They are indicated by gray scale images. From the porosity distribution calculated from Eq. (6), the presence of the packed spheres can be seen and it is found that there is a little space where the fluids pass through. On the other hand, it is shown that the gas phase (white area) moves upward, as shown in the Fig. 5 (b). The test section is filled by the alumina spheres, so the air passes through the narrow gap between spheres. Although it is difficult to track the small bubbles, the move of the large bubble can be found roughly from the void fraction distribution estimated from the radiograph.

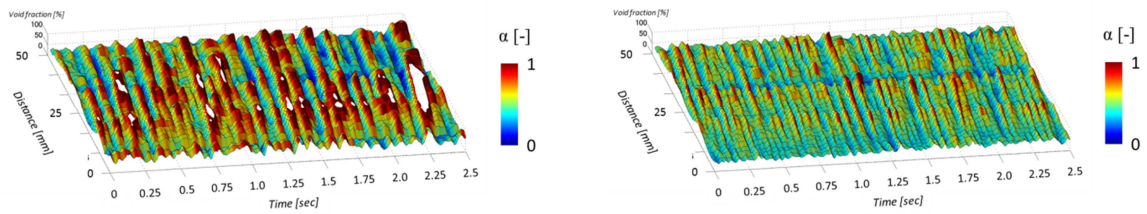

(a) J_L=0.01m/s (b) J_L=0.03m/s

Fig. 6. Spatio-temporal distributions of cross-sectional averaged void fraction at J_G = 0.1 m/s.

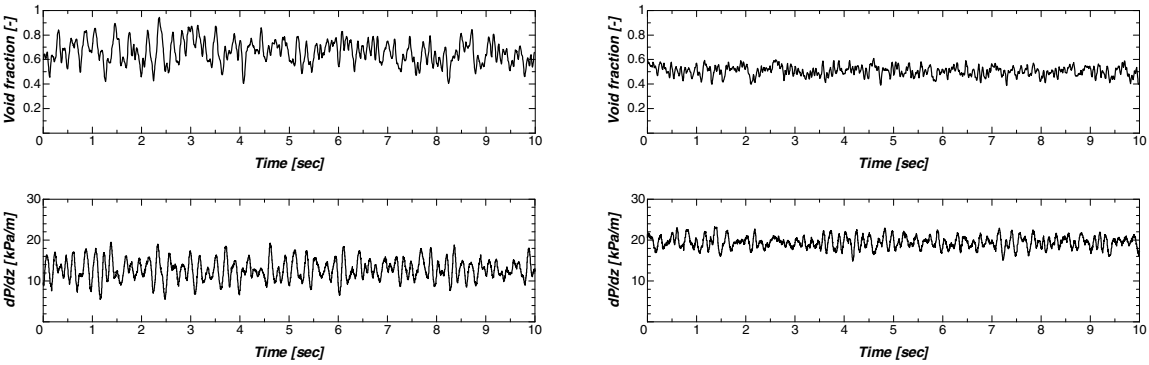

(a) J_L=0.01m/s (b) J_L=0.03m/s

Fig. 7. Comparison between void fraction (upper) and pressure drop (bottom) at J_G = 0.1 m/s.

3.3. Fluctuation of averaged void fraction

Spatio-temporal distributions of the cross-sectional averaged void fraction are shown in Fig. 6. Each axis denotes the time, the axial distance and the void fraction. The void fraction is also indicated by a color map. Many lines formed by the high void fraction value are found in these figures and it is easily seen that bubbles pass through the packed bed. The slope of the lines corresponds to the rising velocity of the bubbles. Relatively large bubbles exist at low superficial liquid velocity, whereas small bubbles flow upward at high superficial liquid velocity. From these figures, the bubble passing frequency at each axial position is also found.

3.4. Comparison with pressure drop

The pressure drop in the test section is measured to compare with the void fraction obtained by the neutron radiography. Comparison results of time-series signals of the void fraction averaged over the test section and the pressure drop are shown in Fig. 7. At lower superficial liquid velocity, large fluctuations are found in both void fraction and pressure drop because the relatively large gas clusters pass through. The amplitude of the fluctuation decreases at higher superficial liquid velocity. This means that a lot of small bubbles flow in the packed bed. From these results, it is shown that the fluctuations of the void fraction and the pressure drop are quite similar and the pressure drop increases with an increase of the superficial liquid velocity. Thus, the two-phase flow structure in the packed bed of the spheres could be understood qualitatively from the void fraction and the pressure drop.

4. Conclusions and future work

In order to establish the experimental database for gas-liquid two-phase flow in the debris bed, measurements of air-water two-phase flow in a packed bed of the spheres were performed by applying the neutron radiography technique. The porosity and void fraction in the porous media were estimated from the radiographs acquired by the dynamic neutron imaging system and the behavior of the gas phase was observed. The fluctuation of the void fraction was compared with that of the pressure drop in the test section. From these results, the possibility of the estimation of the gas velocity and the passing frequency was shown.

The dynamic two-phase flow behavior in the packed bed in the circular pipe was visualized by the high frame-rate neutron radiography in this study. However, more detailed discussions will be done by applying the weighted averaging and Abel conversion to the measured distributions of the porosity and the void fraction. Furthermore, the distribution characteristics in the cross section will be evaluated by applying the CT imaging technique.

References

Duvala, F., Fichota, F., Quintardb, M., 2004. A Local Thermal Non-Equilibrium Model for Two-Phase Flows with Phase-Change in Porous Media. International Journal of Heat and Mass Transfer 47-3, 613-639.

Hibiki, T., Mishima, K., Yoneda, K., Fujine, S., Tsuruno, A., Matsubayashi, M., 1994. Visualization of fluid phenomena using a high frame-rate neutron radiography with a steady thermal neutron beam, Nuclear Instruments and Methods in Physics Research A 351, 423-436.

Kureta, M., Akimoto, H., Hibiki, T., Mishima, K., 2001. Void Fraction Measurement in Subcooled-Boiling Flow using High-Frame-Rate Neutron Radiography, Nuclear Technology 136, 241-254.

Saito, Y., Sekimoto, S., Hino, M., Kawabata, Y., 2011. Development of Neutron Radiography Facility for Boiling Two-Phase Flow Experiment in Kyoto University Research Reactor. Nuclear Instruments and Methods in Physics Research Section A: Accelerators, Spectrometers, Detectors and Associated Equipment 651, 36-41.

Sehgal, B.R., 2011. Nuclear Safety in Light Water Reactors, 1st Edition, Academic Press, New York,

Takenaka, N., Asano, H., Fujii, T., Murata, Y., Mochiki, K., Taguchi, A., Matsubayashi, M., Tsuruno, A., 1996. Void Fraction Distribution Measurement in Two-Phase Flow by Real-Time Neutron Radiography and Real-Time Image Processing. Nuclear Instruments and Methods in Physics Research Section A: Accelerators, Spectrometers, Detectors and Associated Equipment 377, 153-155.

Wang, C.Y., Beckermann, C., 1993. A Two-Phase Mixture Model of Liquid-Gas Flow and Heat Transfer in Capillary Porous Media – I. Formulation. International Journal of Heat and Mass Transfer 36, 2747-2758.